Multispectral photoacoustic imaging of fluorochromes in small animals

Daniel Razansky, Claudio Vinegoni, and Vasilis Ntziachristos*

Center for Molecular Imaging Research, Massachusetts General Hospital, Harvard Medical School, Charlestown, Massachusetts 02129, USA

**Corresponding author: vasilis@helix.mgh.harvard.edu*

Received July 3, 2007; revised August 15, 2007; accepted August 17, 2007; posted August 29, 2007 (Doc. ID 84673); published September 28, 2007

Fluorochromes have become essential reporter molecules in biological research. We show that the depth-resolved distribution of fluorochromes in small animals can be imaged with 25 fmol sensitivity and 150 μm spatial resolution by means of multispectral photoacoustic imaging. The major advantage of the multispectral approach is the sensitive differentiation of chromophores and fluorochromes of interest based on self-reference measurements, as evidenced in this study by resolving a commonly used fluorochrome (Alexa Fluor 750) in mouse. The suggested method is well suited for enhancing visualization of functional and molecular information *in vivo* and longitudinally. © 2007 Optical Society of America

OCIS codes: 170.3880, 170.5120, 170.6280.

Photoacoustic imaging of tissues has demonstrated the ability to resolve common chromophores with spatial resolution exceeding that of ultrasound [1,2]. The method relies on ultrasonic detection of photoacoustically induced signals following absorption of light by tissue chromophores. The amplitude of the generated broadband ultrasound wave reflects local optical absorption properties of tissue. Since scattering of ultrasonic waves in a biological medium is weak, as compared with that of light, biomedical photoacoustic imaging combines high optical absorption contrast with diffraction-limited resolution of ultrasonic imaging. Consequently, hemoglobin-based contrast has been demonstrated by imaging vascular structures [1], blood oxygenation [3], and tumor angiogenesis [4].

While resolving hemoglobin is important for assessing tissue function, the use of extrinsically administered optical agents has recently revolutionized noninvasive photonic imaging by allowing visualization of otherwise invisible cellular and subcellular processes. The use of contrast agents and fluorescent reporters with specificity to proteins and enzymes, for example, has shown a high potential to differentiate several diverse disease biomarkers [5,6]. Photoacoustic imaging has been also applied to imaging exogeneous contrast agents, e.g., light-absorbing nanoshells [7] or chromogenic assays [8].

This study examines for the first time to our knowledge the performance of multispectral photoacoustic imaging (MPI) in resolving biodistribution of fluorescent molecules deep in tissues of small animals. Multispectral methods have been previously shown to be useful in imaging fluorochrome distributions in tissues by optical imaging [9]. In photoacoustics, spectral methods were applied for differentiating blood chromophores [3] and for resolving dyes in nonabsorbing phantoms [2]. Here we suggest the application of MPI as a comprehensive method to provide self-referencing measurements for longitudinal studies over extended periods of times or in molecular imaging studies using commonly available fluorochromes. Fluorophores play an important role in biological research, and there is a large pool of available agents utilized in *in vivo* applications. Fluorescence is further used extensively in correlative fluorogenic assays and microscopy or immunohistochemistry studies. It is then advantageous to noninvasively image fluorescent agents using photoacoustic methods because of their extensive use in biomedical applications. In addition, some fluorochromes, especially in the near IR, possess relatively high molar extinction coefficients in excess of $10^5\ M^{-1}\ cm^{-1}$ in conjunction with low quantum yield (reduced fluorescence efficiency), acting in favor of photoacoustic signal generation. Naturally, the methodology presented herein can be equally applied to imaging pure (nonradiative) chromophores that offer absorption transitions over narrow spectral bands, similarly to fluorochromes.

The experimental setup employed for photoacoustic measurements consists of a tunable optical parametric oscillator laser (Vibrant-532-I, Opotek Inc., Carlsbad, California). The laser pulse duration in the near IR (680–950 nm) was below 10 ns with a pulse repetition frequency of 20 Hz. The beam was expanded, and its diameter on the imaged object was 10 mm. A broadband ultrasonic transducer with central frequency of 3.7 MHz and 75% bandwidth (Model V382, Panametrics-NDT, Waltham, Massachusetts), cylindrically focused in the imaged plane, was used to record the photoacoustic signals transmitted from the imaged object. The time-resolved signals recorded by the transducer were amplified, digitized, and averaged by an embedded oscilloscope card at 100 Msps (NI PCI-5122, National Instruments Corp., Austin, Texas) and 14 bit digital resolution. The laser beam and the transducer were fixed for each data acquisition required for two-dimensional tomographic inversion, whereas the imaged object was rotated 360° with 2° steps by using a rotation stage. For three-dimensional data acquisition, the transducer was also scanned along the vertical axis. The total acquisition time per two-dimensional image slice was 5 min.

0146-9592/07/192891-3/$15.00

MPI was based on measurements at 750, 770, and 790 nm, selected from a larger pool of available wavelengths for demonstration purposes. This range covers the entire declining slope in the excitation spectra of AF750 (Alexa Fluor 750, Invitrogen Corp., Carlsbad, California), a common near-IR fluorescent dye used for labeling in molecular imaging applications [5], which was also used in the current study. Its measured molar extinction spectrum is plotted in Fig. 1 together with the spectra of common tissue chromophores. At 790 nm, the extinction (absorption) coefficient of the fluorochrome becomes negligible; thus measurements at this wavelength served for self-reference. Tomographic inversion was performed separately for each wavelength by using filtered backprojection [1]. In contrast with inversions applied assuming homogeneous light distribution within appropriately selected sections of tissue [1,7,8], the particular inversion scheme applied herein incorporates a diffusive model of photon propagation in tissues, in order to correct the acquired raw RF data for the corresponding intensity drop of the signal due to the light attenuation as a function of propagation distance. To achieve this, the surface of the imaged object is extracted from the photoacoustic images and a finite-element solver is applied to calculate the light intensity distribution within it. The solver assumes uniform illumination conditions on object's surface and average scattering and absorption properties of tissue at the operating wavelengths [10] are assigned to its volume, i.e., $\mu_s' = 10\ \mathrm{cm}^{-1}$ and $\mu_a = 0.3\ \mathrm{cm}^{-1}$, respectively. The reconstructed photoacoustic images are then corrected for the predicted light distribution. Subsequently, the multispectral processing method is applied, fitting the known absorption spectrum of the fluorochrome employed (Fig. 1) to the reconstructed absorption value at each pixel of the photoacoustic images at the different wavelengths. The resulting image therefore reports the intensity of the fitted curve, on a per-pixel basis. Two-dimensional image reconstruction on a dual-core Pentium IV 3.2 GHz processor, having 2 GBytes of RAM, typically required 5 s of computation time, assuming a 256×256 mesh.

For MPI experiments, we injected 250 pmol of AF750 into the pelvic limb of euthanized wild-type BALB/c mice, approximately 5 mm below the knee joint. The imaging sessions were performed immediately after the injection. Euthanasia was performed according to institutionally approved procedures. The limb had an ellipticlike cross section of about 10 mm × 7 mm at the imaging plane and presented a realistic and fairly challenging imaging target owing to the presence of acoustically mismatched impedance of bones as well as realistic tissue optical heterogeneity.

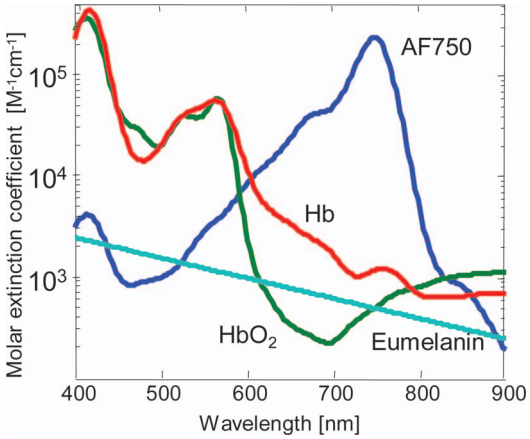

Fig. 1. Wavelength dependence of absorption by AF750 and common tissue chromophores.

The reconstructed photoacoustic images at the three wavelengths, shown in Figs. 2(a)–2(c), attain a similar appearance. The injected fluorochrome is not visible in these images. Correspondingly, spectrally enhanced imaging clearly reconstructs the presence of the fluorochrome, as shown in Figs. 2(d)–2(f). Figures 2(d) and 2(e) depict simpler implementations of the multispectral approach by simply subtracting the image acquired at 790 nm from the 750 and 770 nm images, respectively. Figure 2(f) shows the result of multispectral fitting, and Fig. 2(g) depicts Fig. 2(f) in color, superimposed on Fig. 2(a) printed in gray scale. The multispectral image shows further noise suppression and more accurate localization of the fluorescent dye, compared with the difference images of Figs. 2(d) and 2(e), as is also confirmed by the planar fluorescence image in Fig. 2(h), acquired by using epi-illumination fluorescence imaging of the dissected tissue section at the end of the noninvasive photoacoustic measurements. Although the tissue dissection process yields some shape changes compared with the images acquired noninvasively, the overall location of the fluorescence in Fig. 2(h) coincides well with the MPI results. Finally, Fig. 2(i) shows a confirmatory ultrasonic image, at approximately the same imaging plane, acquired by using a

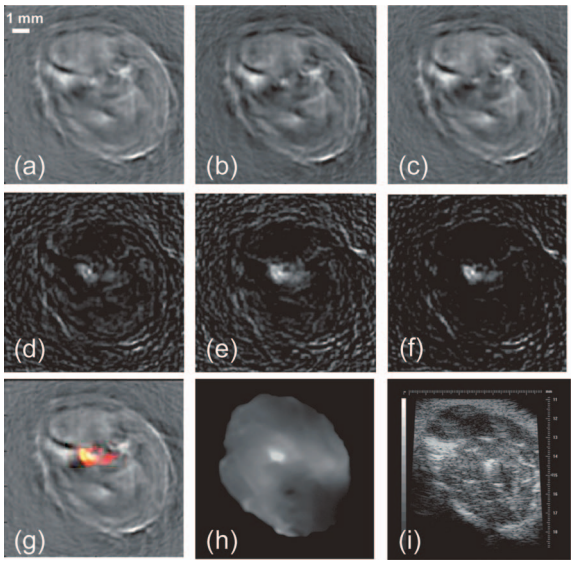

Fig. 2. Photoacoustic tomography cross-sectional images, acquired at (a) 750, (b) 770, and (c) 790 nm. (d) Subtraction between 770 and 790 nm images. (e) Subtraction between 750 and 790 nm images. (f) MPI image incorporating measurements at all three wavelengths. (g) MPI image superimposed onto the photoacoustic image at 750 nm. (h) Planar fluorescence image of the sliced tissue, and (i) corresponding 25 MHz ultrasound image.

VisualSonics Vevo 660TM (VisualSonics Inc., Toronto, Ontario) high-resolution ultrasound imaging system operating at 25 MHz. Apparently, the triangular-shaped *tibia* as well as the *fibula* bones can be seen in both photoacoustic and ultrasound images.

Multispectrally enhanced photoacoustic imaging has been found herein capable of visualizing fluorochromes in tissues that are otherwise not visible at conventional photoacoustic images acquired at single wavelengths. This is achieved without the need for baseline measurements obtained before the administration of the probe. This approach operates optimally by selecting fluorochromes (or possibly chromophores) with a steep drop in their absorption spectrum and selecting, accordingly, the imaging wavelengths to capture this absorption change. When fluorescent dyes are used, the emphasis is on low-quantum-yield fluorochromes, which are particularly useful for photoacoustic signal excitation. The absorption spectrum of AF750 employed here drops significantly in the spectral window 750–790 nm, compared with the smooth absorption variation of the spectra of common tissue chromophores in the near-IR, as shown in Fig. 1. Therefore intrinsic tissue contrast can be readily suppressed with a multispectral approach, yielding highly sensitive imaging of fluorochrome distribution in tissue. While the simplest version of this operation can be achieved by image subtraction at two wavelengths, 3-wavelength and overall multispectral imaging further suppress the background signals as compared with those originating from the AF750 fluorescent dye.

To gain quantitative insights into MPI of tissues, we have calculated the corresponding performance characteristics, given the known system characteristics and the fluorochrome amount injected in the tissue. Correspondingly, for diffraction-limited photoacoustic tomography [7,9], the maximal lateral (in-plane) resolution is determined by the 5 MHz (–6 dB) bandwidth of the transducer employed, resulting in a 150 μm resolution. The vertical resolution in our setup is limited by the focal width of the cylindrically focused transducer to approximately 1.2 mm at 3.7 MHz. We have also calculated the contrast-to-noise ratio of our MPI image in Fig. 2(f) to be above 11. Subsequently, considering the resolution-limited voxel of the approach, i.e., $0.15\ \text{mm} \times 0.15\ \text{mm} \times 1.2\ \text{mm} = 27\ \text{nl}$, and the total volume of the injected AF750 solution (25 μl), the per-unit-volume sensitivity limit is calculated to be $250\ \text{pmol} \times 27\ \text{nl}/11/25\ \mu\text{l} \approx 25\ \text{fmol}$ of AF750. While the *in vivo* situation may yield somewhat different tissue characteristics and noise, which can also reduce the ability to detect activity in a single pixel over noise, the metrics predicted herein evince of a sensitive detection approach for fluorochromes and other absorbers.

By accounting for photon propagation characteristics, MPI was shown for the first time to our knowledge to be appropriate for imaging fluorochromes in real tissues, simultaneously providing the underlining anatomical and functional reference images. Given the great availability and selection of fluorochromes and their probing and targeting mechanisms, the MPI tomography method presented here holds great promise of becoming a valuable high-resolution molecular imaging tool. This is because visualization is achieved by virtually simultaneous measurements at different wavelengths, serving as reference measurements to distinguish otherwise invisible absorbers and fluorochromes in tissues, potentially offering a powerful platform for both functional and molecular imaging. Acquisition at an even larger number of wavelengths could lead to independently resolving multiple absorbers, dyes, and fluorochromes at the expense of longer acquisition times. As compared with most purely absorbing chromophores, having relatively broadband optical absorption characteristics, many fluorochromes exhibit sharp resonances in the vicinity of their peak excitation spectra, an advantageous property for the highly sensitive multispectral imaging approach suggested herein. In addition, the availability of nonradiative contrast agents and molecular probes for photoacoustic imaging is very limited as compared with the large variety of fluorescent molecular markers. Therefore, even though more specific MPI dyes may be developed, imaging of readily available fluorochromes can be achieved at physiologically useful concentrations even in the presence of highly absorbing tissue chromophores. Naturally, both the resolution and the sensitivity of the approach can potentially be improved, depending on the particular tissue and hardware characteristics. The use of ultrasonic detection arrays in photoacoustic measurements [2] or interferometric approaches [11] might further improve the performance and utility of the method in high-throughput imaging applications. Thus, overall, MPI is found to be a highly useful approach for fluorochrome imaging in tissues.

References

1. X. Wang, Y. Pang, G. Ku, G. Stoica, and L. V. Wang, Nat. Biotechnol. **21**, 803 (2003).
2. R. A. Kruger, W. L. Kiser Jr., D. R. Reinecke, G. A. Kruger, and K. D. Miller, Molec. Imag. **2**, 113 (2003).
3. J. Laufer, D. Delpy, C. Elwell, and P. Beard, Phys. Med. Biol. **52**, 41 (2007).
4. R. I. Siphanto, K. K. Thumma, R. G. M. Kolkman, T. G. van Leeuwen, F. F. M. de Mul, J. W. van Neck, L. N. A. van Adrichem, and W. Steenbergen, Opt. Express **13**, 89 (2005).
5. X. Montet, V. Ntziachristos, J. Grimm, and R. Weissleder, Cancer Res. **65**, 6330 (2005).
6. R. M. Hoffman, Lancet Oncol. **3**, 546 (2002).
7. Y. Wang, X. Xie, X. Wang, G. Ku, K. L. Gill, D. P. O'Neal, G. Stoica, and L. V. Wang, Nano Lett. **4**, 1689 (2004).
8. L. Li, R. J. Zemp, G. Lungu, G. Stoica, and L. V. Wang, J. Biomed. Opt. **12**, 020504 (2007).
9. V. Ntziachristos and R. Weissleder, Opt. Lett. **26**, 893 (2001).
10. A. J. Welch and M. J. C. van Gemert, eds., *Optical Thermal Response of Laser-Irradiated Tissue* (Plenum, 1995).
11. B. T. Cox and P. C. Beard, IEEE Trans. Ultrason. Ferroelectr. Freq. Control **54**, 394 (2007).